

# 6FDA-TAPOB Hyperbranched Polyimide-Silica Hybrids for Gas Separation Membranes

Tomoyuki Suzuki, Yasuharu Yamada, Kumi Itahashi

Department of Materials Science and Engineering, Nagoya Institute of Technology, Gokiso-Cho, Showa-Ku, Nagoya 466-8555, Japan

Received 16 October 2007; accepted 26 January 2008

DOI 10.1002/app.28145

Published online 8 April 2008 in Wiley InterScience (www.interscience.wiley.com).

**ABSTRACT:** Physical and gas transport properties of hyperbranched polyimide-silica hybrid membranes were investigated. Hyperbranched polyamic acid as a precursor was prepared by polycondensation of a triamine, 1,3,5-tris(4-aminophenoxy) benzene (TAPOB), and a dianhydride, 4,4'-(hexafluoroisopropylidene)diphthalic anhydride (6FDA), and subsequently modified a part of end groups by 3-aminopropyltrimethoxysilane (APTTrMOS). The hyperbranched polyimide-silica hybrid membranes were prepared by sol-gel reaction using the polyamic acid, water, and alkoxysilanes. 5% weight-loss temperature of the hybrid membranes increased with increasing silica content, indicating effective crosslinking at polymer-silica interface mediated by APTTrMOS moiety. On the other hand, glass transition temperature of the hybrid membranes prepared with methyltrimethoxysilane (MTMS) showed a minimum value at low silica

content region, suggesting insufficient formation of three-dimensional Si—O—Si network compared to the hybrid membranes prepared with tetramethoxysilane (TMOS). CO<sub>2</sub>, O<sub>2</sub>, N<sub>2</sub>, and CH<sub>4</sub> permeability coefficients of the hybrid membranes increased with increasing silica content. Especially for TMOS/MTMS combined system, the hybrid membranes showed simultaneous enhancements of gas permeability and CO<sub>2</sub>/CH<sub>4</sub> separation ability. It was concluded that the 6FDA-TAPOB hyperbranched polyimide-silica hybrid membranes have high thermal stability and excellent CO<sub>2</sub>/CH<sub>4</sub> selectivity and are expected to apply to high-performance gas separation membranes. © 2008 Wiley Periodicals, Inc. *J Appl Polym Sci* 109: 813–819, 2008

**Key words:** hyperbranched polyimide; silica hybrid; gas separation

## INTRODUCTION

Gas separation processes using polymer membranes have greatly been developed during the last three decades. Especially polyimides have been of great interest in gas separation membranes because of their high gas selectivity and excellent thermal and mechanical properties. In this regard, a large number of polyimides have been studied about their gas transport properties.<sup>1–4</sup> In the recent years, novel triamine-based hyperbranched polyimides (HBPIs) have been synthesized and characterized to investigate their potential for high-performance gas separation materials. Fang et al.<sup>5,6</sup> have synthesized HBPIs derived from a triamine, tris(4-aminophenyl)amine, and commercially available dianhydrides and studied their physical and gas transport properties, and it has been shown that the HBPIs have good gas separation performance compared to linear-type polyimides. In our previous study, gas transport properties of the HBPI prepared by polycondensation of a triamine, 1,3,5-tris(4-aminophenoxy)benzene

(TAPOB), and a dianhydride, 4,4'-(hexafluoroisopropylidene)diphthalic anhydride (6FDA) have been investigated, and it has been found that the 6FDA-TAPOB HBPI exhibits high gas permeability and O<sub>2</sub>/N<sub>2</sub> selectivity arising from the characteristic hyperbranched structure.<sup>7</sup>

Organic-inorganic hybrids are attractive materials because they generally possess desirable organic and inorganic properties. Hybridization with inorganic compounds has been focused on the modification of polyimides to improve their thermal, mechanical, and gas transport properties.<sup>8–10</sup> In our previous reports, gas transport properties of several HBPI-silica hybrid membranes prepared by sol-gel reaction using tetramethoxysilane (TMOS) have been investigated, and it has been found that gas permeability and CO<sub>2</sub>/CH<sub>4</sub> selectivity of the HBPI-silica hybrid membranes increase with increasing silica content, suggesting characteristic distribution and interconnectivity of free volume holes created by the incorporation of silica.<sup>11–13</sup> Thus far, the HBPI-silica hybrid membranes were prepared using TMOS, there are no data for gas transport properties of the hybrid membranes prepared with different kinds of alkoxysilanes.

In this work, physical and gas transport properties of 6FDA-TAPOB HBPI-silica hybrid membranes prepared by sol-gel method with two kinds of alkoxysi-

Correspondence to: Y. Yamada (yamada.yasuharu@nitech.ac.jp).

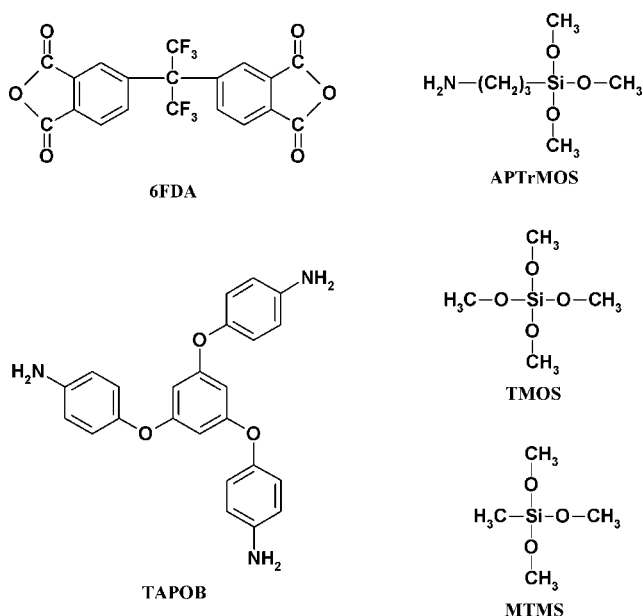


**Figure 1** Chemical structures of monomers and alkoxysilanes.

lanes, TMOS and methyltrimethoxysilane (MTMS), individually or simultaneously, are investigated. The methyl group of MTMS will prevent the formation of robust three-dimensional Si—O—Si network in the hybrid membranes. It is expected the loose Si—O—Si network induces unique physical and gas transport properties of the hybrid membranes.

## EXPERIMENTAL

### Materials

TAPOB was synthesized by the reduction of 1,3,5-tris(4-nitrophenoxy)benzene with palladium carbon and hydrazine in methanol.<sup>14</sup> 6FDA was kindly supplied from Daikin Industries. TMOS, MTMS, and 3-aminopropyltrimethoxysilane (APTrMOS) were purchased from Aldrich. Chemical structures of monomers and alkoxysilanes are shown in Figure 1.

### Polymerization

Three millimolars of 6FDA were dissolved in 40 mL of *N,N*-dimethylacetamide (DMAc) in a 100-mL three-necked flask under N<sub>2</sub> flow at room temperature. To this solution, 1.6 mmol of TAPOB in 20 mL of DMAc was added dropwise through a syringe with stirring for 3 h. After that, 0.4 mmol of APTTrMOS was added in the reaction mixture with stirring for 1 h to afford 6FDA-TAPOB hyperbranched polyamic acid.

### Membrane formation

The 6FDA-TAPOB HBPI-silica hybrid membranes were prepared by sol-gel reaction with two kinds of

alkoxysilanes, TMOS and/or MTMS, and thermal imidization. Appropriate amounts of TMOS and/or MTMS and water were added in the DMAc solution of the hyperbranched polyamic acid. For TMOS/MTMS combined system, TMOS and MTMS were added to achieve equivalent weight fraction of silica components arising from TMOS and MTMS. The mixed solutions were stirred for 24 h and cast on PET films and dried at 85°C for 3 h. The prepared membranes were peeled off and subsequently imidized at 100°C for 1 h, 200°C for 1 h, and 300°C for 1 h in a heating oven under N<sub>2</sub> flow. Average thickness of the HBPI-silica hybrid membranes was about 30 μm.

### Measurements

Infrared (IR) spectra were recorded on a JASCO FTIR-460 plus. Ultraviolet (UV)-vis optical transmittances were investigated by a JASCO V-530 UV-vis spectrometer at a wavelength of 200–800 nm. Thermo-gravimetric-differential thermal analysis (TG-DTA) experiments were performed with a Seiko TG/DTA6300 at a heating rate of 10°C/min under air flow. Thermal mechanical analysis (TMA) measurements were undergone using a Seiko TMA/SS6100 at a heating rate of 5°C/min under N<sub>2</sub> flow. CO<sub>2</sub>, O<sub>2</sub>, N<sub>2</sub>, and CH<sub>4</sub> permeation measurements were carried out by a constant volume/variable pressure apparatus at 76 cmHg and 25°C. The permeability coefficient,  $P$  [cm<sup>3</sup>(STP)cm/cm<sup>2</sup> s cmHg], was determined by the following equation<sup>15</sup>;

$$P = \frac{22414 L V dp}{A p RT dt} \quad (1)$$

where  $A$  is the membrane area (cm<sup>2</sup>),  $L$  is the membrane thickness (cm),  $p$  is the upstream pressure (cmHg),  $V$  is the downstream volume (cm<sup>3</sup>),  $R$  is the universal gas constant (6236.56 cm<sup>3</sup> cmHg/mol K),  $T$  is the absolute temperature (K), and  $dp/dt$  is the permeation rate (cmHg/s). The gas permeability coefficient can be explained on the basis of the solution-diffusion mechanism, which is represented by the following equation<sup>16,17</sup>;

$$P = D \times S \quad (2)$$

where  $D$ (cm<sup>2</sup>/s) is the diffusion coefficient and  $S$  [cm<sup>3</sup>(STP)/cm<sup>3</sup><sub>polym</sub> cmHg] is the solubility coefficient. The diffusion coefficient was calculated by the time-lag method represented by the following equation<sup>18</sup>;

$$D = \frac{L^2}{6\theta} \quad (3)$$

where  $\theta$  (s) is the time-lag.

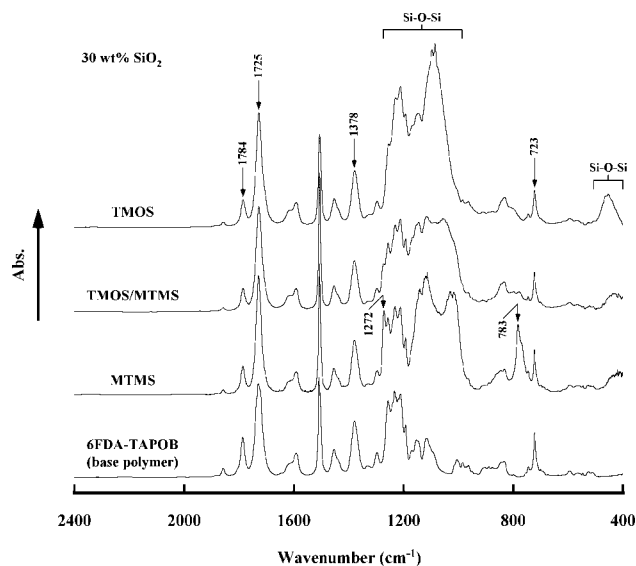


**Figure 2** FTIR spectra of 6FDA-TAPOB HBPI-silica hybrid membranes (silica content = 30 wt %).

## RESULTS AND DISCUSSION

### Polymer characterization

FTIR spectra of the 6FDA-TAPOB HBPI-silica hybrid membranes, containing 30 wt % of silica, prepared with various alkoxyxilanes are shown in Figure 2. The bands observed around  $1784\text{ cm}^{-1}$  (C=O asymmetrical stretching),  $1725\text{ cm}^{-1}$  (C=O symmetrical stretching),  $1378\text{ cm}^{-1}$  (C–N stretching), and  $723\text{ cm}^{-1}$  (C=O bending) are characteristic absorption bands of polyimides.<sup>6,19</sup> In contrast, the characteristic band of polyamic acids around  $1680\text{ cm}^{-1}$  is not found. These results indicate that the prepared membranes are well imidized. For MTMS and TMOS/

TMOS combined systems, the bands around  $1272$  and  $783\text{ cm}^{-1}$ , assigned to Si–CH<sub>3</sub> stretching and rocking, respectively,<sup>9</sup> are also observed. The absorption bands at  $\sim 960$ – $1280$  and  $410$ – $480\text{ cm}^{-1}$ , identified as asymmetric stretching and rocking modes of the Si–O–Si group, respectively<sup>9,20</sup> are observed, indicating the formation of Si–O–Si network in the hybrid membranes. For the TMOS system, the strong absorption bands of the Si–O–Si asymmetric stretching appear around  $1180$  and  $1090\text{ cm}^{-1}$ . On the other hand, for the MTMS system, they appear around  $1120$  and  $1030\text{ cm}^{-1}$  with the red shift in turn to a lower wavenumber. The red shift of the absorption bands reveals decreasing bonding energy and increasing bond distance of the bond between Si and O atoms in the Si–O–Si network.<sup>20</sup> Therefore, for the MTMS system, the red shift of the Si–O–Si peaks suggests the formation of a looser silica network caused by the methyl group in MTMS, which function as a terminating substituent in the formation of Si–O–Si bonds to perturb microstructure of resulting silica matrix. In addition, it is pointed out that the absorption bands of the Si–O–Si asymmetric stretching for the TMOS/MTMS combined system are the overlap of those for TMOS and MTMS systems, suggesting the formation of Si–O–Si network with an intermediate structure.

Optical transmittances of the hybrid membranes are shown in Table I. It can be said that the hybrid membranes have a high homogeneity because of their good transparency similarly to pure 6FDA-TAPOB HBPI without silica. The high homogeneity is considered to be maintained not only by APTRMOS moiety, which functions as covalent bond parts between organic and inorganic components but also

**TABLE I**  
Physical Properties of 6FDA-TAPOB HBPI–Silica Hybrid Membranes

Sample	Transmittance <sup>a</sup> (%)	$T_g$ (°C)	$T_d^5$ (°C)	Silica content <sup>b</sup> (wt %)	CTE <sup>c</sup> (ppm/°C)	
6FDA-TAPOB	88.9	282	457	0	54	
TMOS	10 wt % SiO <sub>2</sub>	89.9	305	490	10	47
	20 wt % SiO <sub>2</sub>	90.2	311	496	20	38
	30 wt % SiO <sub>2</sub>	90.3	318	509	30	31
	40 wt % SiO <sub>2</sub>	90.3	318	509	30	31
TMOS/MTMS	10 wt % SiO <sub>2</sub>	89.6	286	487	10	50
	20 wt % SiO <sub>2</sub>	90.1	299	494	18	48
	30 wt % SiO <sub>2</sub>	89.8	301	502	29	46
	40 wt % SiO <sub>2</sub>	89.1	303	509	40	41
	50 wt % SiO <sub>2</sub>	91.6	n.d. <sup>d</sup>	515	48	–
MTMS	10 wt % SiO <sub>2</sub>	90.2	278	471	10	59
	20 wt % SiO <sub>2</sub>	90.1	281	480	19	66
	30 wt % SiO <sub>2</sub>	91.4	287	496	30	73
	40 wt % SiO <sub>2</sub>	91.3	291	501	39	74
	50 wt % SiO <sub>2</sub>	91.7	n.d. <sup>d</sup>	505	48	–

<sup>a</sup> Optical transmittance at 600 nm.

<sup>b</sup> Determined from the residual at 800°C.

<sup>c</sup> CTE at 100–150°C.

<sup>d</sup> Not detected.

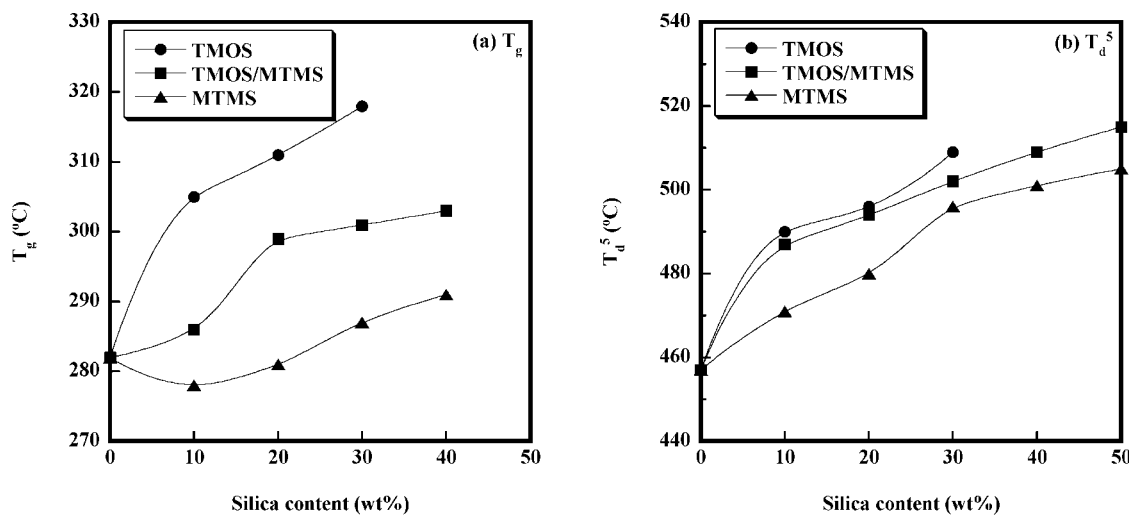


**Figure 3** (a) Glass transition temperature ( $T_g$ ) and (b) 5% weight-loss temperature ( $T_d^5$ ) of 6FDA-TAPOB HBIP-silica hybrid membranes plotted against silica content.

by the characteristic hyperbranched structure of molecular chains.<sup>21</sup>

Thermal properties of the hybrid membranes were investigated by TG-DTA and TMA measurements. From thermogravimetric curves, it was again demonstrated that the prepared membranes are well imidized, because no weight-losses attributed to dehydration by imidization are observed all through the measurements. Glass transition temperatures ( $T_g$ s) determined from DTA curves and 5% weight-loss temperatures ( $T_d^5$ s) of the hybrid membranes are summarized in Table I in addition to the silica content determined from the residual at 800°C. It is confirmed from the residual that all hybrid membranes contain appropriate amount of silica as expected. The  $T_g$  and  $T_d^5$  values of the hybrid membranes are plotted against silica content in Figure 3.  $T_d^5$ s of the hybrid membranes increase with increasing silica content. This result indicates the increase in thermal stability of the HBPI matrix by hybridization with silica. The  $T_g$  of the TMOS system considerably increases with increasing silica content, suggesting the formation of robust three-dimensional Si—O—Si network. However, for the MTMS system, the  $T_g$  shows a minimum value at low silica content region, and the  $T_g$  of the TMOS/MTMS combined system is lower than that of the TMOS system. This fact suggests that the introduction of MTMS leads to an insufficient formation of three-dimensional Si—O—Si network, which brings about less constraint of molecular chains in the hybrid membranes compared to the case of hybrid membranes prepared solely with TMOS.

Coefficients of thermal expansion (CTEs) from 100 to 150°C of the hybrid membranes are listed in Table I. The CTE of the TMOS system greatly decreases with increasing silica content, indicating the enhancement of thermal mechanical stability of the HBPI matrix by

the formation of robust three-dimensional Si—O—Si network. In contrast, the CTE of the MTMS system increases with increasing silica content. The increased CTE might be caused by a loose Si—O—Si network, which induces an effective disruption of molecular chains packing and, as a result, provides a large amount of free volume holes.<sup>22</sup> The increased free volume holes decrease the hindrance of thermal expansion of molecular chains. The CTE of the TMOS/MTMS combined system shows the intermediate value between those of TMOS and MTMS systems.

#### Gas transport properties of 6FDA-tapob hbpi-silica hybrid membranes

Gas permeability, diffusion, and solubility coefficients of the 6FDA-TAPOB HBPI-silica hybrid membranes are summarized in Table II. Gas permeability coefficients of the hybrid membranes increase with increasing silica content. The increased permeability suggests additional formation of free volume holes effective for gas transport behaviors. Similar enhancement of free volume holes has been reported by Merkel et al. for high-free-volume, glassy polymer-nanosilica composites, and they have concluded that the nanosilica particles yield polymer/particle interfacial area and provided disruption of polymer chain packing and affect gas transport behaviors.<sup>23,24</sup> He et al. have also reported that nanosized inorganic fillers incorporated into high-free-volume, glassy polymers with rigid molecular chains can function as a spacer material, which disrupts molecular chain packing, leading to increases in fractional free volume and gas permeability.<sup>25</sup> It is worth noting, for MTMS and TMOS/MTMS combined systems, significant improvements of gas permeability mainly caused by the increased diffusivity are observed. It

**TABLE II**  
**Gas Transport Properties of 6FDA-TAPOB HBPI—Silica Hybrid Membranes at 76 cmHg and 25°C**

Sample	$P \times 10^{10}$ (cm <sup>3</sup> (STP)cm/cm <sup>2</sup> s cmHg)				$D \times 10^8$ (cm <sup>2</sup> /s)				$S \times 10^2$ (cm <sup>3</sup> (STP)/ cm <sup>3</sup> polym cmHg)				
	CO <sub>2</sub>	O <sub>2</sub>	N <sub>2</sub>	CH <sub>4</sub>	CO <sub>2</sub>	O <sub>2</sub>	N <sub>2</sub>	CH <sub>4</sub>	CO <sub>2</sub>	O <sub>2</sub>	N <sub>2</sub>	CH <sub>4</sub>	
6FDA-TAPOB	7.4	1.5	0.23	0.098	0.30	1.4	0.25	0.028	25	1.1	0.92	3.5	
TMOS	10 wt % SiO <sub>2</sub>	10	2.0	0.31	0.13	0.35	1.5	0.29	0.026	30	1.4	1.1	5.0
	20 wt % SiO <sub>2</sub>	13	2.1	0.32	0.16	0.37	1.3	0.25	0.030	35	1.7	1.3	5.2
	30 wt % SiO <sub>2</sub>	23	3.0	0.46	0.24	0.57	1.7	0.29	0.040	41	1.8	1.6	6.0
TMOS/MTMS	10 wt % SiO <sub>2</sub>	13	2.7	0.41	0.20	0.59	2.1	0.46	0.060	22	1.3	0.90	3.3
	20 wt % SiO <sub>2</sub>	28	5.4	0.89	0.45	1.2	4.0	0.90	0.090	24	1.4	1.0	4.9
	30 wt % SiO <sub>2</sub>	44	7.9	1.3	0.74	1.7	5.9	1.2	0.17	26	1.3	1.2	4.4
	40 wt % SiO <sub>2</sub>	72	12	2.3	1.4	2.6	7.9	1.8	0.25	27	1.5	1.3	5.5
	50 wt % SiO <sub>2</sub>	133	22	4.5	2.8	5.2	14	3.7	0.63	26	1.6	1.2	4.4
MTMS	10 wt % SiO <sub>2</sub>	23	4.4	0.75	0.45	1.0	3.8	0.83	0.13	23	1.2	0.90	3.6
	20 wt % SiO <sub>2</sub>	53	9.5	1.9	1.5	2.6	8.7	2.2	0.42	21	1.1	0.90	3.7
	30 wt % SiO <sub>2</sub>	99	18	4.1	4.1	5.4	16	4.8	1.2	19	1.1	0.86	3.4
	40 wt % SiO <sub>2</sub>	158	28	7.6	10	9.9	28	9.3	3.7	16	1.0	0.82	2.7
	50 wt % SiO <sub>2</sub>	251	46	14	20	17	46	17	6.8	15	1.0	0.79	3.0

is well known that the gas diffusivity of polymers strongly depends on the total fractional free volume.<sup>26,27</sup> Therefore, the enormous improvements of gas diffusivity suggest large enhancements of mean size and total amount of free volume holes attributed to the loose Si—O—Si networks for MTMS and TMOS/MTMS combined systems.

#### O<sub>2</sub>/N<sub>2</sub> and CO<sub>2</sub>/CH<sub>4</sub> selectivities of 6FDA-TAPOB HBPI-silica hybrid membranes

The ideal gas selectivity for the combination of gases A and B [ $\alpha(A/B)$ ] is defined by the following equation<sup>28</sup>;

$$\alpha(A/B) = \frac{P(A)}{P(B)} = \frac{D(A)}{D(B)} \times \frac{S(A)}{S(B)} = \alpha^D(A/B) \times \alpha^S(A/B) \quad (4)$$

where  $\alpha^D(A/B)$  is the diffusivity selectivity and  $\alpha^S(A/B)$  is the solubility selectivity. The O<sub>2</sub>/N<sub>2</sub> and CO<sub>2</sub>/CH<sub>4</sub> selectivities of the hybrid membranes are listed in Table III, and  $\alpha(O_2/N_2)$  and  $\alpha(CO_2/CH_4)$  are plotted against O<sub>2</sub> and CO<sub>2</sub> permeability coefficients, respectively (Figs. 4 and 5).

In Figure 4, it is recognized that the  $\alpha(O_2/N_2)$  values of the hybrid membranes slightly decrease with increasing O<sub>2</sub> permeability along with the upper bound trade-off line for O<sub>2</sub>/N<sub>2</sub> separation demonstrated by Robeson.<sup>29</sup> This behavior is consistent with the general understanding that polymers, which are more permeable, are less selective and vice versa. Nevertheless, it seems the potential of O<sub>2</sub>/N<sub>2</sub> separation ability of pure 6FDA-TAPOB HBPI is kept maintaining because the hybrid membranes show relatively high  $\alpha(O_2/N_2)$  values just below the upper bound.

**TABLE III**  
**O<sub>2</sub>/N<sub>2</sub> and CO<sub>2</sub>/CH<sub>4</sub> Selectivities of 6FDA-TAPOB HBPI—Silica Hybrid Membranes at 76 cmHg and 25°C**

Sample	O <sub>2</sub> /N <sub>2</sub> selectivity			CO <sub>2</sub> /CH <sub>4</sub> selectivity			
	$\alpha(O_2/N_2)$	$\alpha^D(O_2/N_2)$	$\alpha^S(O_2/N_2)$	$\alpha(CO_2/CH_4)$	$\alpha^D(CO_2/CH_4)$	$\alpha^S(CO_2/CH_4)$	
6FDA-TAPOB	6.8	5.8	1.2	75	11	7.0	
TMOS	10 wt % SiO <sub>2</sub>	6.6	5.2	1.3	79	13	5.9
	20 wt % SiO <sub>2</sub>	6.7	5.3	1.3	82	12	6.8
	30 wt % SiO <sub>2</sub>	6.6	5.8	1.1	95	14	6.7
TMOS/MTMS	10 wt % SiO <sub>2</sub>	6.6	4.7	1.4	65	9.9	6.6
	20 wt % SiO <sub>2</sub>	6.0	4.4	1.4	62	13	4.9
	30 wt % SiO <sub>2</sub>	5.9	5.1	1.2	59	10	5.9
	40 wt % SiO <sub>2</sub>	5.2	4.4	1.2	53	11	5.0
	50 wt % SiO <sub>2</sub>	5.0	3.7	1.3	48	8.2	5.8
MTMS	10 wt % SiO <sub>2</sub>	5.9	4.5	1.3	51	8.1	6.3
	20 wt % SiO <sub>2</sub>	4.9	4.0	1.2	34	6.0	5.6
	30 wt % SiO <sub>2</sub>	4.3	3.4	1.3	24	4.4	5.4
	40 wt % SiO <sub>2</sub>	3.7	3.0	1.2	15	2.7	5.8
	50 wt % SiO <sub>2</sub>	3.4	2.6	1.3	12	2.5	4.9

For CO<sub>2</sub>/CH<sub>4</sub> separation, attractive behaviors are observed (Fig. 5). The  $\alpha(\text{CO}_2/\text{CH}_4)$  of the hybrid membranes prepared solely with TMOS increases with increasing silica content in connection with increased CO<sub>2</sub> permeability. The remarkable CO<sub>2</sub>/CH<sub>4</sub> separation behavior of the 6FDA-TAPOB HBPI-silica hybrid membranes prepared with TMOS is considered to be due to characteristic distribution and interconnectivity of free volume holes created by the incorporation of silica, which provides a size-selective CO<sub>2</sub>/CH<sub>4</sub> separation ability.<sup>11</sup> On the other hand, the  $\alpha(\text{CO}_2/\text{CH}_4)$  of the MTMS system decreases with increasing CO<sub>2</sub> permeability as similar as the cases of conventional polymeric membranes as described earlier. The distinctive difference between TMOS and MTMS systems is considered to be due to the differences in mean size and total amount of free volume holes created by the incorporation of silica. The size-selective CO<sub>2</sub>/CH<sub>4</sub> separation ability of the hybrid membranes prepared with MTMS is sacrificed by excess enhancements of mean size and total amount of free volume holes although CO<sub>2</sub> permeability of the MTMS system is markedly increased. It should be noted that the CO<sub>2</sub>/CH<sub>4</sub> separation ability of the TMOS/MTMS combined system shows an intermediate behavior between those of TMOS and MTMS systems. As shown in Figure 5, the  $\alpha(\text{CO}_2/\text{CH}_4)$  of the TMOS/MTMS combined system maintains in a high state and tends to exceed the upper bound for CO<sub>2</sub>/CH<sub>4</sub> separation<sup>29</sup> with increasing CO<sub>2</sub> permeability or silica content. Although similar tendency of improvement of CO<sub>2</sub>/CH<sub>4</sub> separation ability has been reported for some linear-type polyimide-silica hybrids,<sup>9</sup> such unique improvements of both CO<sub>2</sub> permeability and CO<sub>2</sub>/

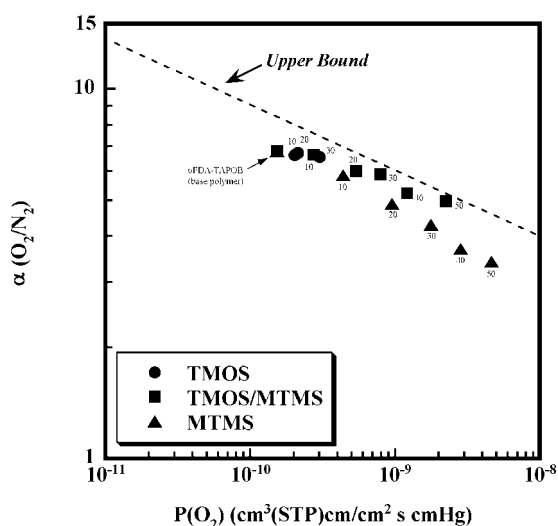


**Figure 4** Ideal O<sub>2</sub>/N<sub>2</sub> selectivity [ $\alpha(\text{O}_2/\text{N}_2)$ ] of 6FDA-TAPOB HBPI-silica hybrid membranes plotted against O<sub>2</sub> permeability coefficient.

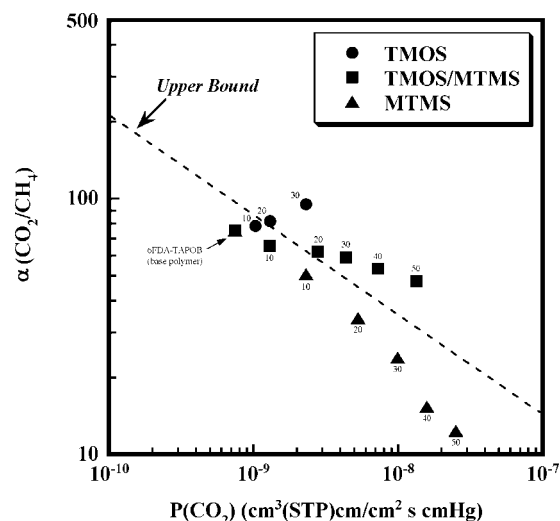


**Figure 5** Ideal CO<sub>2</sub>/CH<sub>4</sub> selectivity [ $\alpha(\text{CO}_2/\text{CH}_4)$ ] of 6FDA-TAPOB HBPI-silica hybrid membranes plotted against CO<sub>2</sub> permeability coefficient.

CH<sub>4</sub> separation ability for the TMOS/MTMS combined system observed in this study have not been reported. This fact indicates mean size and distribution of free volume holes in the TMOS/MTMS combined system are successfully controlled and, as a result, the TMOS/MTMS combined system shows simultaneous large enhancements of CO<sub>2</sub> permeability and CO<sub>2</sub>/CH<sub>4</sub> separation ability.

## CONCLUSIONS

Physical and gas transport properties of 6FDA-TAPOB HBPI-silica hybrid membranes prepared by sol-gel method with two kinds of alkoxy silanes, TMOS and MTMS, were investigated. From the comparison of FTIR spectra for the TMOS and MTMS systems, the red shift of the Si—O—Si peaks is observed for the hybrid membranes prepared with MTMS, suggesting the formation of a looser Si—O—Si network caused by the methyl group in MTMS, which induces large enhancements of mean size and total amount of free volume holes compared to the TMOS system. The enhanced free volume holes bring a minimum  $T_g$  at low silica content region and increased CTE for the MTMS system. CO<sub>2</sub>, O<sub>2</sub>, N<sub>2</sub>, and CH<sub>4</sub> permeability coefficients of the hybrid membranes increase with increasing silica content because of additional formation of free volume holes. In particular, MTMS and TMOS/MTMS combined systems show enormous improvements of gas diffusivity because of large enhancements of mean size and total amount of free volume holes attributed to the loose Si—O—Si networks. The TMOS/MTMS combined system also exhibits simultaneous large enhancements of CO<sub>2</sub> permeability

and CO<sub>2</sub>/CH<sub>4</sub> separation ability. This fact indicates mean size and distribution of free volume holes in the TMOS/MTMS combined system are successfully controlled to achieve the unique size-selective CO<sub>2</sub>/CH<sub>4</sub> separation ability. Finally, it is concluded that the 6FDA-TAPOB HBPI-silica hybrid membranes have excellent gas separation ability and are expected to apply to high-performance gas separation membranes.

## References

1. Sykes, G. F.; Clair, A. K. S. *J Appl Polym Sci* 1986, 32, 3725.
2. Okamoto, K.; Tanaka, K.; Kita, H.; Ishida, M.; Kakimoto, M.; Imai, Y. *Polym J* 1992, 24, 451.
3. Langsman, M.; Burgoyne, W. F. *J Polym Sci Part A: Polym Chem* 1993, 31, 909.
4. Li, Y.; Wang, X.; Ding, M.; Xu, J. *J Appl Polym Sci* 1996, 61, 741.
5. Fang, J.; Kita, H.; Okamoto, K. *Macromolecules* 2000, 33, 4639.
6. Fang, J.; Kita, H.; Okamoto, K. *J Membr Sci* 2001, 182, 245.
7. Suzuki, T.; Yamada, Y.; Tsujita, Y. *Polymer* 2004, 45, 7167.
8. Cornelius, C. J.; Marand, E. *J Membr Sci* 2002, 202, 97.
9. Hibshman, C.; Cornelius, C. J.; Marand, E. *J Membr Sci* 2003, 211, 25.
10. Hibshman, C.; Mager, M.; Marand, E. *J Membr Sci* 2004, 229, 73.
11. Suzuki, T.; Yamada, Y. *J Polym Sci Part B: Polym Phys* 2006, 44, 291.
12. Suzuki, T.; Yamada, Y.; Sakai, J. *High Perform Polym* 2006, 18, 655.
13. Suzuki, T.; Yamada, Y. *High Perform Polym* 2007, 19, 553.
14. Takeichi, T.; Stille, J. K. *Macromolecules* 1986, 19, 2093.
15. Prabhakar, R. S.; Freeman, B. D.; Roman, I. *Macromolecules* 2004, 37, 7688.
16. Muruganandam, N.; Koros, W. J.; Paul, D. R. *J Polym Sci Part B: Polym Phys* 1987, 25, 1999.
17. Morisato, A.; Shen, H. C.; Sankar, S. S.; Freeman, B. D.; Pinnau, I.; Casillas, C. G. *J Polym Sci Part B: Polym Phys* 1996, 34, 2209.
18. Weinkauff, D. H.; Kim, H. D.; Paul, D. R. *Macromolecules* 1992, 25, 788.
19. Chen, H.; Yin, J. *J Polym Sci Part A: Polym Chem* 2002, 40, 3804.
20. Zhu, H.; Ma, Y.; Fan, Y.; Shen, J. *Thin Solid Films* 2001, 397, 95.
21. Tomokiyo, N.; Yamada, Y.; Suzuki, T.; Oku, J. *Polym Prep Japan* 2006, 55, 5175.
22. Smiaili, M.; Jermoumi, T.; Marignan, J.; Noble, R. D. *J Membr Sci* 1996, 116, 211.
23. Merkel, T. C.; Freeman, B. D.; Spontak, R. J.; He, Z.; Pinnau, I.; Meakin, P.; Hill, A. *J Sci* 2002, 296, 519.
24. Merkel, T. C.; Toy, L. G.; Andraday, A. L.; Gracz, H.; Stejskal, E. O. *Macromolecules* 2003, 36, 353.
25. He, Z.; Pinnau, I.; Morisato, A. In *Advanced Materials for Membrane Separation*; Pinnau, I.; Freeman, B. D., Eds.; ACS Symposium Series 876; American Chemical Society: Washington, DC, 2004; pp 218–233.
26. Park, J. Y.; Paul, D. R. *J Membr Sci* 1997, 125, 23.
27. Thran, A.; Kroll, G.; Faupel, F. J. *J Polym Sci Part B: Polym Phys* 1999, 37, 3344.
28. Freeman, B. D. *Macromolecules* 1999, 32, 375.
29. Robeson, L. M. *J Membr Sci* 1991, 62, 165.